Toward Nanometer-Scale Resolution in Fluorescence Microscopy Using Spectral Self-Interference

Anna K. Swan, Lev A. Moiseev, C. R. Cantor, Brynmor Davis, S. B. Ippolito, William Clem Karl, Bennett B. Goldberg, and M. Selim Ünlü, *Senior Member, IEEE*

***Abstract*—We introduce a new fluorescence microscopy technique that maps the axial position of a fluorophore with subnanometer precision. The interference of the emission of fluorophores in proximity to a reflecting surface results in fringes in the fluorescence spectrum that provide a unique signature of the axial position of the fluorophore. The nanometer sensitivity is demonstrated by measuring the height of a fluorescein monolayer covering a 12-nm step etched in silicon dioxide. In addition, the separation between fluorophores attached to the top or the bottom layer in a lipid bilayer film is determined. We further discuss extension of this microscopy technique to provide resolution of multiple layers spaced as closely as 10 nm for sparse systems.**

***Index Terms*—Fluorescence microscopy, interference, spectroscopy, ultra high-optical resolution.**

I. Introduction

HIGH-RESOLUTION fluorescence microscopy is a central tool in cell and molecular biology, since visible light probes living cells noninvasively. Its versatility is due to the large selection of fluorescent markers combined with their specificity in staining. In addition to revolutionizing structural studies, functional studies have been made possible by the varying responses of fluorescent tags to local environments and the use of green fluorescent protein and its derivatives as fusion-protein tracers.

A significant constraint of light microscopy is the limitation of spatial resolution due to diffraction that is proportional to wavelength λ and inversely proportional to numerical aperture ($NA = n\sin\theta$, where n is the refractive index in the object space, and θ is the half-angle subtended). Diffraction-limited resolution can be improved by increasing the *NA*, as in 4Pi-confocal microscopy [1]–[3], and using oil- or water-immersion objectives. Of course, reducing the wavelength also increases resolution [4], but the high energies are generally incompatible with live cells. There are several ways in which the resolution can be improved beyond the diffraction limit in fluorescence microscopy due to the specific nature of fluorescence. Two-photon microscopy achieves very high signal-to-noise ratio compared to confocal microscopy, since the excitation probability is proportional to the square of the intensity [5]. However, since the wavelength is twice as large, compared to conventional confocal microscopy, the resolution is not greatly improved. Fluorescence microscopy by standing-wave excitation [6] exploits interference in the excitation optical field to create a periodic modulation. Scanning the standing wave, collecting fluorescence, and subsequent deconvolution [7] yield sub-100-nm axial resolution as well as improved lateral resolution [8], [9]. In addition, both emission and excitation interferences have also been exploited by placing the fluorophores atop a reflecting substrate. A very accurate axial height determination is achieved by analyzing the change in overall emission intensity with varying fluorophore-to-reflecting-mirror distance [10]–[12]. Combining wide-field collection with interference in the emission and excitation, as in I^5M, leads to axial resolution better than 100 nm [13], [14]. Hell and co-workers used the stimulated emission depletion (STED) technique to quench the fluorescence surrounding a very small volume, thus, effectively increasing the resolution in both lateral and axial directions to $\sim$ 100 nm [15], [16]. Recently, they combined the use of 4Pi microscopy with STED and achieved an unprecedented optical resolution of 33 nm, currently the world record [17].

In this paper, we show experimental results that demonstrate a new interferometric technique in fluorescent imaging we call spectral self-interference fluorescence microscopy. The technique determines the axial position down to less than a nanometer using the spectral signature of fluorescent markers placed above a reflecting surface. Furthermore, we discuss how to proceed in order to resolve an axial distribution of fluorophores on the scale of 10 nm.

II. Spectral Self-Interference Fluorescence Microscopy

For many years, scientists have recognized that fluorophore emission is affected by the proximity of dielectric or metal surfaces. Energy transfer, excitation field standing wave, and interference in the emission all lead to significant changes in fluorescence emission. Thirty years ago, Drexhage utilized organic dyes on stepped multilayer Langmuir-Blodgett films above a mirror to measure fluorescence lifetime as a function of distance from the mirror and found an oscillatory dependence on the distance [18], [19]. These results are due to the simple fact

Manuscript received December 11, 2002; revised February 10, 2003. This work was supported in part by the National Science Foundation under Grant DBI-0128425 and in part by Corning, Inc.

A. K. Swan, B. Davis, S. B. Ippolito, W. C. Karl, and M. S. Ünlü are with the Electrical and Computer Engineering Department, Boston University, Boston, MA 02215 USA (e-mail: swan@bu.edu; bryn@bu.edu; ippolito@bu.edu; wckarl@bu.edu; selim@bu.edu).

L. Moiseev is with the Biology Department, Boston University, Boston, MA 02215 USA (e-mail: leva1@bu.edu).

C. R. Cantor is with the Biomedical Engineering Department, Boston University, Boston, MA 02215 USA (e-mail: ccantor@sequenom.com).

B. B. Goldberg is with the Physics Department and Electrical and Computer Engineering Department, Boston University, Boston, MA 02215 USA (e-mail: goldberg@bu.edu).

Digital Object Identifier 10.1109/JSTQE.2003.814191

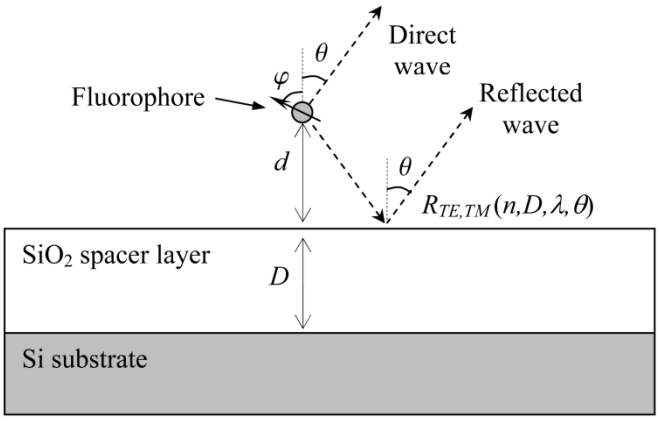

Fig. 1. Schematic drawing of the geometrical arrangement of the fluorophore and the reflective substrate. The complex reflection coefficient $R_{\mathrm{TE,TM}}$ contains the effect of the multiple reflections from the top and bottom of the SiO2 interfaces. Note that d is enlarged relative to D in the figure for clarity. The silicon dioxide spacer layer thickness D is typically 5 μm, while d is a few nanometers

that when the fluorophore is within $\sim \lambda$ of the reflecting surface, the entire emission spectrum is enhanced or quenched as the direct and reflected emitted light undergoes constructive or destructive interference as a function of the vertical distance.

Spectral self-interference fluorescence microscopy is based on a similar model, but interrogates the spectral intensity distribution of interference fringes instead of the variation of intensity with height. It also requires a different configuration of the substrate: the separation between the fluorophore and the reflecting substrate is much greater than λ, typically 10 wavelengths. Fig. 1 schematically shows the configuration for the setup. Note that, while d is the dimension of interest in the nanometer scale, the spacer layer thickness D is large (on the order of 10 wavelengths) and the dominant reflection takes place at the SiO_2-Si interface. A long path length difference between direct and reflected light means that only a small change in the wavelength is needed to go from constructive to destructive interference. The effect of the long path difference is included in the wavelength-dependent reflection coefficient R defined for the system. The result is oscillations, or fringes, in the emission spectrum—a unique spectral signature of the height of the emitter above the reflector. Small height differences produce shifts in the fringes and changes in the period of oscillation, although the latter are less apparent. The broader the emission spectrum, the more information is collected and the more precise the height determination. The distance above the mirror can be determined solely from the oscillations within the spectrum [20], [21]. Tanigushi *et al.* [22] observed this type of oscillations for a broad distribution of vertical positions of fluorophores and found a qualitative agreement with data using a classical model of self-interference of the spontaneous emission. It is important to recognize that, in contrast to approaches using fluorescence interference contrast microscopy [10]–[12], the axial position of the fluorophores in our technique is encoded in the spectral oscillations and not in the overall intensity. Therefore, variations in fluorophore density, emission intensity, and the excitation field strength will not affect the determination of axial position.

III. Experimental Setup

The experimental setup consists of a commercial microscope with a laser port to couple illumination for excitation and an attached spectrometer with a cooled charged coupled device (CCD) camera for spectroscopy. The substrates are polished silicon wafers with a $\sim$ 5-μm-thick oxide layer grown by plasma-enhanced chemical vapor deposition (PECVD) [23]. The lipid bilayer study was performed on wafers that were chemo-mechanically polished to a measured RMS roughness of less than 2 nm following PECVD. To reference the fluorescence location to the top of the silicon dioxide layer and to find the precise thickness D of the oxide spacer layer, white light reflectivity measurements are performed (Fig. 1). The white light reflectivity measurements use a standard halogen lamp integral to the microscope (Kohler illumination configuration).

The emitters in our experiments are fluorescein isothiocyanate (FITC) or CdSe quantum dots capped with ZnS. The fluorophores are excited by the 488-nm line of an argon ion laser focused onto the sample with a $5\times$ objective. The fluorescence emission is collected through the excitation path and separated from the laser by a 488-nm holographic notch filter. The emission is focused on an entrance slit to the spectrometer, dispersed by an 1800 grove/mm grating, and recorded on the CCD (spectral resolution 2 cm^{-1}). Monolayers of fluorescein (FITC) were immobilized on the SiO_2 surfaces via isothiocyanate-aminosilane chemistry. ZnS-capped quantum dots were treated with mercaptoacetic acid to make them water-soluble and negatively charged at neutral pH, and then electrostatically attached to aminosilane (APTES)-treated SiO_2 surfaces.

The lipid in Langmuir–Blodgett films is dipalmitoyl phosphatidylethanolamine (DPPE). The fluorescently labeled layer contains 2:100 molar ratio of fluorescein dihexadecanoyl phosphatidylethanolamine (f-DHPE) added to DPPE before deposition.

The sample with embedded quantum dots used was prepared by immobilizing quantum dots on top of the SiO_2 spacer layer and covering the sample with an additional layer of $\sim$ 40 nm SiO_2 by electron-beam evaporation technique in a vacuum chamber with base pressure $5 \bullet 10^{-7}$ Torr. The height position of the quantum dots was verified by white light interference measurements before immobilizing the quantum dots as well as by fluorescence measurements. The dots have been chosen so as to have a large size distribution, causing a broad emission band (preferred) shown in Fig. 2(b).

On our flat reflecting substrates, we use a low numerical aperture (*NA*) objective ($5\times$, $NA = 0.12$) in order to limit the collection to a small cone. For high numerical aperture objectives, integration over large collection angles washes out the interference fringes due to different path lengths corresponding to constructive and destructive interference for the same wavelength. In addition, for the white light measurements, the condenser aperture diaphragm is reduced to its minimum, resulting in a maximum illumination angle of 1.36°. Hence, using flat substrates achieves a very precise height determination at the expense of a low light collection efficiency and low lateral resolution. It is possible to retain nm-scale axial resolution while using

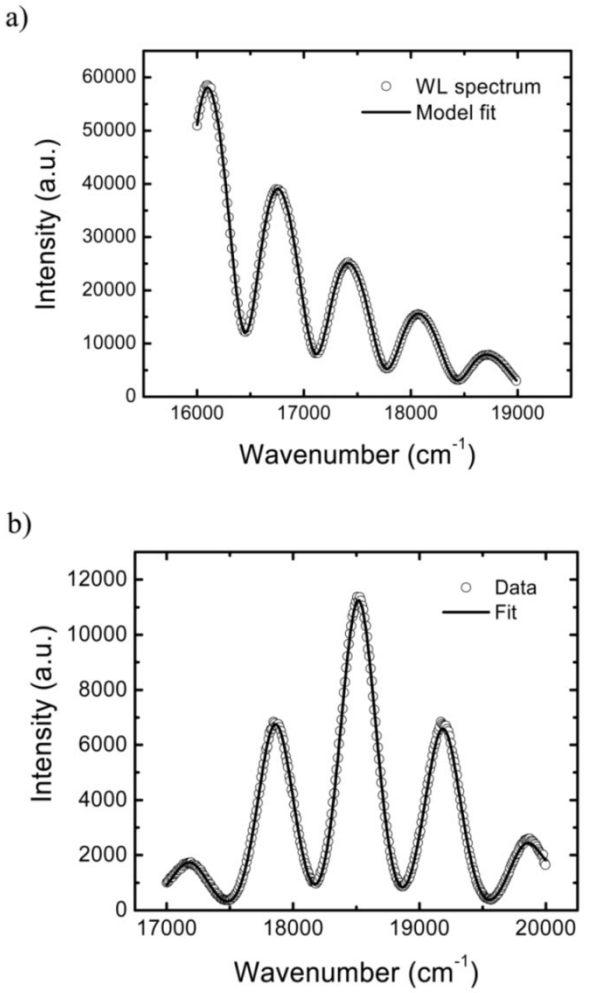

Fig. 2. (a) Measured and fitted white light reflectivity spectrum. (b) Measured spectrum from quantum dots embedded in SiO_2 with fluorescence interference model fit.

a high-*NA* objective, with the accompanying high lateral resolution and light collection efficiency, by utilizing a spherical micromirror as the reflector. The downwardly emitted phase fronts are spherical at the mirror surface and are reflected exactly back to the point of origin, removing any angular dependence of the phase difference between the direct and reflected light.

IV. Data Analysis

A. White Light Fitting Procedure

The optical thickness of a thin film can be measured accurately by white light reflectivity interference spectroscopy, since the white light spectrum contains spectral fringes due to the multiple reflections from the two interfaces. This technique has more recently been used as a label-free method for monitoring biomolecular interactions [24]. Here, we have used white light reflectivity interference to measure the precise thickness of the silicon dioxide spacer and the optical thickness of a lipid bilayer film.

The intensity fringes in the spectrum are given by the reflectivity $|R|^2$, where $R(R_{\mathrm{TE}}, R_{\mathrm{TM}},)$ is the total reflection coefficient of the dielectric layers. The reflection coefficient for the two interfaces in our system is calculated using the matrix propagation method for different wavelengths and angles of incidence [25], [26]. It is necessary to take into account both the wavelength dispersion of the index of refraction $n = n(\lambda)$ for all dielectric layers and the imaginary part k of the index of refraction of silicon. The measured spectrum is fitted with a calculated spectrum where the only unknown is D—the thickness of the oxide spacer layer. The fitted spectrum coincides very well with the measured spectrum as shown in Fig. 2(a). The absolute accuracy of the measurements depends upon the knowledge of the index of refraction; we are using index of refraction data for stoichiometric SiO_2 that may deviate slightly ($\sim 10^{-4}$) from the actual index of refraction.

B. Analysis of Fluorescence Interference

A fluorescent marker located at distance d above the spacer layer is excited by laser light introduced through the microscope to the sample. The fluorescence emission spectrum depends on three major components: 1) the excitation intensity at the given fluorophore height due to the standing wave of the laser excitation light which scales the overall intensity of the fluorescence emission; 2) the smooth emission spectrum envelope of a free fluorophore, which forms the envelope of the spectral fringe pattern; and 3) the interference between direct and reflected emission, which creates the spectral fringe pattern that holds all of the height information. The interference component of the intensity for each emitter is given by

$$\left|E_{\mathrm{TM,TE}}(\theta,\varphi,\psi) + E_{\mathrm{TM,TE}}(\pi-\theta,\varphi,\psi)R_{\mathrm{TM,TE}}(n,D,\lambda,\theta)e^{-ik2d\cos\theta}\right|^2. \quad (1)$$

$E_{\mathrm{TM,TE}}$ is the far-field amplitude of the electric field emitted by the dipole in a given direction; θ is the collection angle; ψ and φ are the polar and the azimuthal orientation angles of the dipole respectively; D is the thickness of the oxide layer; and d is the height of the fluorophore above the surface. $R_{\mathrm{TE,TM}}$ is the total (complex) reflection coefficients for the transverse electric (TE) and transverse magnetic (TM) field components for the dielectric mirror stack, i.e., the silicon dioxide/silicon structure. The reflection coefficients include $n(\lambda)D$—the optical path in the silicon dioxide spacer layer. The white light data provides the thickness, D. The emission intensity is integrated over the cone defined by the numerical aperture of the objective ($5\times$, $NA = 0.12$). The only unknown parameters are d the height of the emitter above the surface and ψ the polar orientation of the dipole. The polar orientation of the dipole affects the contrast of the fringes and the overall intensity; no net azimuthal angle is expected due to the azimuthal symmetry of the sample.

In the calculations above, there are two simplifying assumptions. First, near-field radiation is ignored, since the observation point is located in the far field. Second, by calculating the reflection coefficients used in (1) with the matrix propagation method, we implicitly assume plane waves for each angle of incidence. We believe this is a reasonable approximation, since the primary mirror surface—the SiO_2/Si interface—is far away from the fluorophore and only a small solid angle is collected. It is also supported by the good agreement between data and the fitting shown in Fig. 2(b).

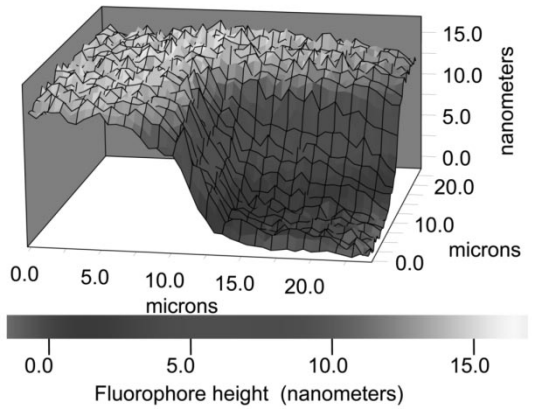

Fig. 3. Spectral self-interference image of fluorescein on a step-etched silicon oxide layer atop silicon. The image shown is a false-color map also rendered as a surface topographic image. Note that the false-color scale corresponds to the height of the fluorescent emitter; the actual emission intensity is uniform.

V. Results

Several experiments have been carried out to assess the validity of the physical model and the sensitivity of the axial height determination using spectral self-interference fluorescence microscopy. To evaluate the sensitivity of height determination we fabricated a grid pattern of small height variations etched into the surface of our ~ 5 μm thick SiO_2/Si substrate. Monolayers of fluorescein (FITC) were immobilized on the SiO_2 surfaces via isothiocyanate-aminosilane chemistry. The surface height variation was mapped both by white light reflectivity and by fitting the emission spectra of surface-bound fluorescein and was found to be in agreement. A spectrum was collected with a $5\times$ objective, $NA = 0.12$, (spot size ~ 3 μm) at each point by scanning the microscope stage in lateral steps of 1 μm. In order to form a height image, the data was analyzed using the model discussed above, so that each spectrum yielded a local height. Fig. 3 displays the height data as a 3-D, false color image of the etched SiO_2 corner, where it is apparent that nanometer scale vertical height determination has been obtained.

In addition, we used self-interference fluorescence microscopy to determine the axial position of fluorophores attached to the head groups of a lipid bilayer film deposited on Si/SiO_2 chips by the Langmuir-Blodgett technique. The fluorescent label was bound either to the top or the bottom layer of the lipids, but not to both layers simultaneously. White light reflectivity measurements were taken before and after lipid layer deposition. The difference of the heights from the top interface to the SiO_2/Si interface yields the thickness of the lipid layer, assuming the lipid layer has an index of refraction close to that of silicon dioxide ($n = 1.462$ at $\lambda = 500$ nm). By measuring the fluorescence response, the location of the fluorophores in the lipid layer can be determined. Fig. 4(a) shows the schematic experimental arrangement of a lipid bilayer (~ 5 nm) deposited on a silicon chip with a thick silicon oxide spacer layer (~ 5 μm). A typical fluorescence spectrum from such layers is shown in Fig. 4(b). Separate measurements were made for fluorophores attached to the top or the bottom leaflet of the lipid bilayer, respectively. For each case, measurements were collected from the same several points, separated

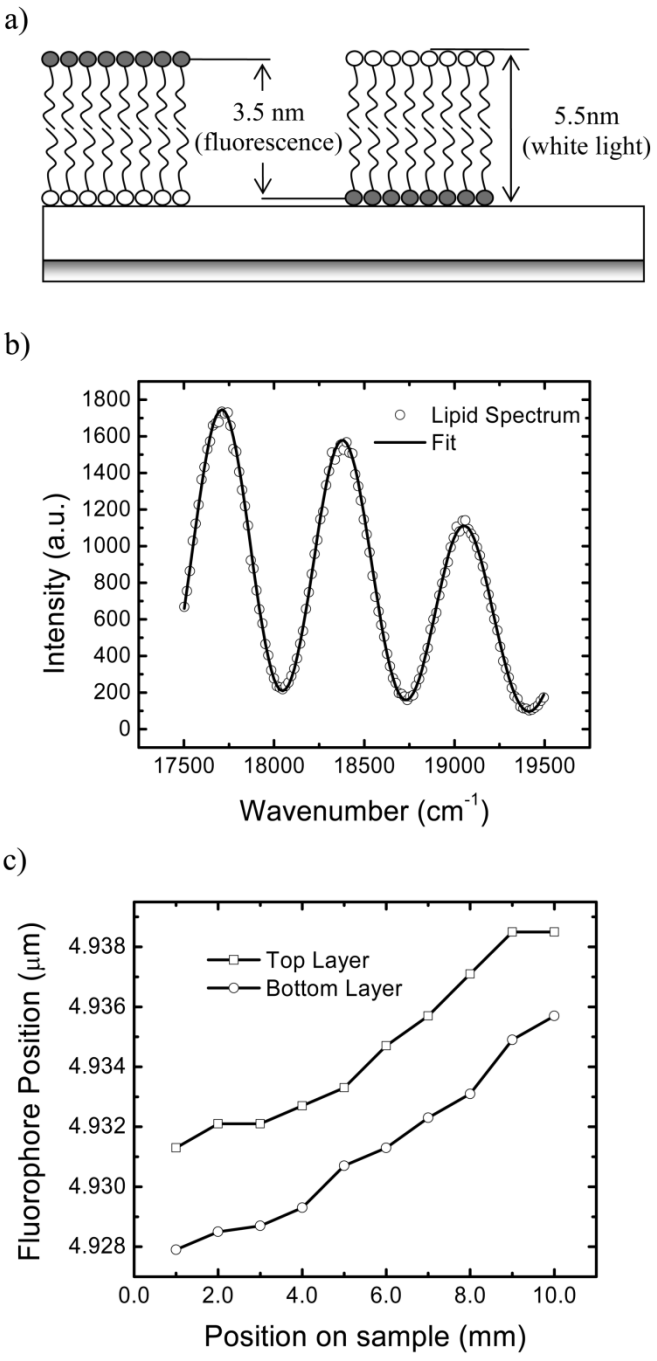

Fig. 4. (a) Schematic picture of the lipid bilayer film systems (not to scale). The figure illustrates two different configurations with fluorophore in the top layer (left) and the bottom layer (right). (b) Representative fluorophore spectrum with along with the fitted model spectrum. (c) Measured fluorophore axial positions across the chip for top and bottom labeling, respectively, determined by spectral self-interference microscopy. The separation of fluorophores in top and bottom layer is the difference between the two measurements. The overall slope of 8 nm/10 mm is due to a slight variation of the thickness of the SiO2 layer across the chip.

by 1 mm, along a line across the sample. The point-to-point registry between measurements is achieved by using fiduciary marks on the sample, and by using the microscope motorized scanning stage, with 5-μm sample-to-sample repeatability. The results are shown in Fig. 4(c). The 10-nm variation in the measured heights across the chip seen in Fig. 4(c) is due

to the variation of the spacer thickness D across the length of the surface scan ($\sim$ 10 mm), as verified by white light reflectivity measurements. As can be seen from Fig. 4(c), the average separation between the fluorophores in the top and the bottom layer is 3.4 ± 0.3 nm. From white light reflectivity measurements, we find the thickness of the lipid layer to be 5.3 ± 0.3 nm. Further studies of the lipid system are currently underway.

VI. Discussion

The spectral self-interference technique described above determines the axial position of fluorophores above a reflecting surface. Our initial measurements from a fluorescein-covered etched corner (Fig. 3) show a significant height variation of several nanometers that, we have discovered, stems from an uneven substrate. The surface height variation on the lateral scale of the spot size (~ 3 μm) was subsequently measured to be ~ 30 nm using atomic force microscopy. On the other hand, the lipid layer was grown on samples prepared by chemomechanical polishing specifically to reduce the roughness of the oxide layer to ~ 2 nm or less on a lateral scale of microns. The measured uniformity from both the white light reflectivity and fluorescence measurements shows a very small variation of 0.3 nm. Considering the residual surface roughness of more than 1 nm, the accuracy of the measurements is quite satisfactory.

VII. Resolving Multiple Axial Positions

The method described above determines the position of a single fluorophore layer. An important generalization would be to determine the positions and relative intensities of several layers. Even for a two-layer system, this is a nontrivial task. To illustrate this, consider the addition of the intensity from the two layers. Since the emission spectrum is close to a sine wave, two closely spaced layers appear nearly as if the resulting spectrum comes from a single layer at the average position. Fig. 5(a) shows simulated data of quantum dot emission (a forward model calculation) from two equally intense quantum dot layers separated by 10 nm, as well as the data that would be produced by a single layer at the average of the heights. Although the difference between the two emission spectra (the residue) is small, it is clearly visible as shown in the inset in Fig. 5(a) and (b). The plot in Fig. 5(b) also includes a Fourier-filtered residue where the filtering has been used to remove the high-frequency components of the Poisson noise in order to make the structure in the residue more visible. The fact that a two-layer system is distinguishable from a one-layer system suggests that inverting the spectral data is possible, if challenging, for at least some systems with more than one layer.

Inverting a two-layer system requires the estimation of four parameters—the position and intensity of each layer. An inversion procedure has been developed and tested in simulations for this two-layer case. For each pair of possible fluorophore positions a corresponding optimal pair of amplitudes can be calculated. As the emission spectra intensities from the two layers add up, this is a simple weighted least-squares problem (where

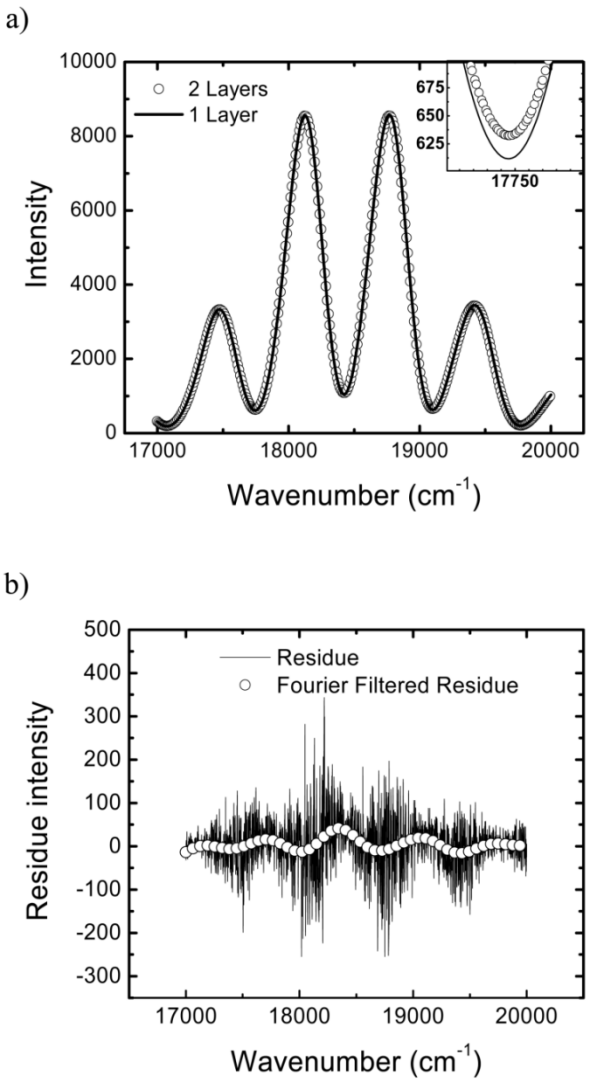

Fig. 5. Resolution simulations. (a) A spectrum originating from two fluorophore layers separated by 10 nm and its best fit assuming only a single fluorophore layer. Notice the small but visible difference between the spectra shown in the inset. (b) The difference between the spectra from these two- and one-layered structures is shown as the residue. Aside from the added Poisson noise which averages to zero, the Fourier filtering of the residue clearly shows the difference in spectra from a single layer and two closely-spaced layers.

the weighting takes into account the changing variance of the Poisson noise at different total photon counts), which can be solved in closed form. This process results in candidate emission spectra for each pair of position parameters. These can be exhaustively searched for the emission spectra closest to that observed—the corresponding four parameters define the estimated fluorophore distribution. In simulations, this approach works for layers spaced down to 5 nm. This performance can be improved by incorporating measurements at multiple excitation standing wave positions. These results show the potential to invert multilayer systems from such interference data.

To tackle multiple layer systems, where the axial fluorophore distribution is not known *a priori*, the sought after fluorophore distribution can be discretized to a number of vertical slices and the inversion problem posed in a simple matrix form. Let the column vector $c(d_n, \theta_m)$ be the emission spectra expected from

a unit intensity fluorophore layer at position d_n and measured using a standing wave with phase position θ_m. The elements of this vector are obtained from (1) and include the effects of the overall system envelope, including both the fluorophore bandwidth and the system response. A data vector y can be constructed by concatenating the measurements from each standing wave position. This data vector can be related to the intensity at each layer (the column vector x) by the following:

$$y = \begin{bmatrix} c(d_1,\theta_1) & c(d_2,\theta_1) & \cdots & c(d_N,\theta_1) \\ c(d_1,\theta_2) & c(d_2,\theta_2) & \cdots & c(d_N,\theta_2) \\ \vdots & \vdots & \ddots & \vdots \\ c(d_1,\theta_M) & c(d_2,\theta_M) & \cdots & c(d_N,\theta_M) \end{bmatrix} \quad x = Cx. \tag{2}$$

The inversion method is used to estimate the fluorophore distribution x from the data y. This is significantly more difficult than inverting a two-layer fluorophore distribution and requires very accurate modeling of the overall emission envelope and system response. The system matrix C depends on many physical system parameters and also the discretization regime chosen. At high resolution (fine discretization), C will also have a significant nullspace, which indicates that there will be patterns of fluorophore distribution unobservable in the data. Although this means the inverse problem is ill-posed, such difficulties can be overcome through inclusion of prior knowledge concerning the underlying fluorophore distribution—that is, through the regularization of the inverse problem [27], [28]. For example, in many applications the fluorophore distribution is known to be sparse (i.e., the number of emitting layers is limited to less than half of the interrogated layers). There are techniques which take this sparsity of the unknown distribution into account and focus the information in the data onto the best reconstruction with this sparseness property [29]. Other prior knowledge of the fluorophore distribution may be similarly included into the inversion process to stabilize the estimate. These are topics of active investigation by the authors.

VIII. Summary

We have demonstrated that the new technique of spectral self-interference fluorescence microscopy can determine the height of a fluorophore above a reflecting surface with nanometer precision. Measurements of a lipid bilayer grown by the Langmuir–Blodgett technique on a SiO_2/Si chip show that, while the lipid film is 5.3 ± 0.3-nm-thick, the separation of fluorophores in the top and bottom layers is 3.4 ± 0.3 nm. Data inversion on simulated data indicates that resolution of a sparse axial distribution on the order of 10 nm is possible.

Acknowledgment

Prof. S. Nie is gratefully acknowledged for providing the CdSe/ZnS quantum dots in these studies. A. K. Swan, M. S. Ünlü, and B. B. Goldberg acknowledge Renishaw Inc.

References

[1] S. W. Hell and E. H. K. Stelzer, "Properties of a 4Pi confocal fluorescence microscope," *J. Opt. Soc. Amer. A*, vol. 9, pp. 2159–2166, 1992.

[2] S. W. Hell, E. H. K. Stelzer, S. Lindek, and C. Cremer, "Confocal microscopy with an increased detection aperture—Type-B 4Pi confocal microscopy," *Opt. Lett.*, vol. 19, pp. 222–224, 1994.

[3] M. Schrader, K. Bahlmann, G. Giese, and S. W. Hell, "4Pi-confocal imaging in fixed biological specimens," *Biophys. J.*, vol. 75, pp. 1659–1668, 1998.

[4] S. Vogt, G. Schneider, A. Steuernagel, J. Lucchesi, E. Schulze, D. Rudolph, and G. Schmahl, "X-ray microscopic studies of the Drosophila dosage compensation complex," *J. Struct. Biol.*, vol. 132, pp. 123–132, 2000.

[5] P. T. C. So, C. Y. Dong, B. R. Masters, and K. M. Berland, "Two-photon excitation fluorescence microscopy," *Annu. Rev. Biomed. Eng.*, vol. 2, pp. 399–429, 2000.

[6] B. Bailey, D. L. Farkas, D. L. Taylor, and F. Lanni, "Enhancement of axial resolution in fluorescence microscopy by standing-wave excitation," *Nature*, vol. 366, pp. 44–48, 1993.

[7] V. Krishnamurthi, B. Bailey, and F. Lanni, "Image processing in 3D standing-wave fluorescence microscopy," *Proc. SPIE*, vol. 2655, pp. 18–25, 1996.

[8] R. Heintzmann and C. Cremer, "Laterally modulated excitation microscopy: Improvement of resolution using a diffraction grating," *Proc. SPIE*, vol. 3568, pp. 185–196, 1998.

[9] G. Cragg and P. T. C. So, "Lateral resolution enhancement with standing evanescent waves," *Opt. Lett.*, vol. 25, pp. 46–48, 2000.

[10] A. Lambacher and P. Fromherz, "Fluorescence interference-contrast microscopy on oxidized silicon using a monomolecular dye layer," *Appl. Phys. A-Mater.*, vol. 63, pp. 207–216, 1996.

[11] D. Braun and P. Fromherz, "Fluorescence interference-contrast microscopy of cell adhesion on oxidized silicon," *Appl. Phys. A-Mater.*, vol. 65, pp. 341–348, 1997.

[12] ——, "Fluorescence interferometry of neuronal cell adhesion on microstructured silicon," *Phys. Rev. Lett.*, vol. 81, pp. 5241–5244, 1998.

[13] M. G. L. Gustafsson, D. A. Agard, and J. W. Sedat, "Sevenfold improvement of axial resolution in 3D widefield microscopy using two objective-lenses," *Proc. SPIE*, vol. 2412, pp. 147–156, 1995.

[14] ——, "(IM)-M-5: 3D widefield light microscopy with better than 100 nm axial resolution," *J. Microsc.-Oxford*, vol. 195, pp. 10–16, 1998.

[15] T. A. Klar, S. Jakobs, M. Dyba, A. Egner, and S. W. Hell, "Fluorescence microscopy with diffraction barrier broken by stimulated emission," *P. Nat. Acad. Sci. USA*, vol. 97, pp. 8206–8210, 2000.

[16] T. A. Klar, M. Dyba, and S. W. Hell, "Stimulated emission depletion microscopy with an offset depleting beam," *Appl. Phys. Lett.*, vol. 78, pp. 393–395, 2001.

[17] M. Dyba and S. W. Hell, "Focal spots of size $\lambda/23$ open up far-field fluorescence microscopy at 33 nm axial resolution," *Phys. Rev. Lett.*, vol. 88, art. no. 163901-1–163901-4, 2002.

[18] K. H. Drexhage, "Monomolecular layers and light," *Scientif. Amer.*, vol. 6, pp. 108–119, 1970.

[19] ——, "Interaction of light with monomolecular dye layers," *Prog. Opt.*, vol. 12, pp. 163–232, 1974.

[20] S. H. Lipoff, W. C. Karl, B. B. Goldberg, M. S. Ünlü, A. K. Swan, L. Moiseev, and Y. Tong, "High resolution spectral self-interference fluorescence microscopy," *Proc. SPIE*, vol. 4621, pp. 77–85, 2002.

[21] A. Swan, M. S. Ünlü, Y. Tong, B. B. Goldberg, L. A. Moiseev, and C.R. Cantor, "Self-interference fluorescent emission microscopy – 5 nm vertical resolution," in *Lasers and Electro-Optics Eur. Tech. Dig*, 2001, pp. 360–361.

[22] H. Taneguchi and H. Ito, "Observation of reflection-induced light correlation in spontaneous emission in front of a mirror," *Opt. Lett.*, vol. 19, pp. 1565–1567, 1994.

[23] *Concept 1*, Microsystems Technol. Labs, Mass. Inst. Technol., Cambridge, MA.

[24] C. Hanel and G. Gauglitz, "Comparison of reflectometric interference spectroscopy with other instruments for label-free optical detection," *Anal. Bioanal. Chem.*, vol. 372, pp. 91–100, 2002.

[25] H. A. Macleod, *Thin-Film Optical Filters*, 2nd ed, H. Angus, Ed. New York: McGraw-Hill, 1989.

[26] P. Yeh, *Optical Waves in Layered Media*. New York: Wiley, 1988.

[27] H. W. Engl, M. Hanke, and A. Neubauer, *Regularization of Inverse Problems*. Norwell, MA: Kluwer, 1996.

[28] C. Vogel, *Computational Methods for Inverse Problems*. Philadelphia, PA: SIAM, 2002.

[29] D. L. Donoho, I. M. Johnstone, J. C. Hoch, and A. S. Stern, "Maximum entropy and the nearly black object," *J. Roy. Statist. Soc. B*, vol. 54, pp. 41–81, 1992.

Anna K. Swan was born in Säffle, Sweden, in 1961. She received the Masters degree in physics engineering from Chalmers University, Gothenburg, Sweden and the Ph.D. degree in physics from Boston University, Boston, MA, in 1994.

She joined the Solid State Division, Oak Ridge National Laboratory, Oak Ridge, TN, as a Wigner Fellow. In 1999, she joined the Electrical and Computer Engineering Department, Boston University, as a Research Assistant Professor. Her research topics are clustered around high spatial resolution spectroscopy. Her active topics are spectral self interference as a means of improving fluorescence microscopy resolution, resonant Raman studies of single carbon nanotubes, and very sensitive and high spatial resolution stress-measurements in micro-electromechanical systems (MEMS) using micro-Raman spectroscopy.

Prof. Swan received two student awards, the Nottingham Prize, and the Morton M. Traum Award for her dissertation on spin-ordering on NiO(100) surfaces using metastable He* scattering.

Lev Moiseev received the B.S. degree in chemistry from Moscow State University, Moscow, Russia, in 1992. He is currently pursuing the Ph.D. degree in biochemistry and molecular biology at Boston University, Boston, MA.

C. R. Cantor, photograph and biography not available at the time of publication.

Brynmor Davis received the B.E. degree (Hons. 1) in electrical engineering from the University of Canterbury, New Zealand, in 1999 and the M.S. degree in electrical and computer engineering from the University of Arizona, Tucson, in 2001. He is currently pursuing the Ph.D. degree in electrical and computer engineering at Boston University, Boston, MA.

His research interests include inverse problems, statistical signal processing, and applications in optics and acoustics.

S. B. Ippolito, photograph and biography not available at the time of publication.

William Clem Karl received the Ph.D. degree in electrical engineering and computer science from the Massachusetts Institute of Technology, Cambridge, in 1991, where he also received the S.M., E.E., and S.B. degrees.

He was a Staff Research Scientist with the Brown-Harvard-M.I.T. Center for Intelligent Control Systems and the M.I.T. Laboratory for Information and Decision Systems, from 1992 to 1994. He joined the faculty of Boston University in 1995, where he is currently an Associate Professor of electrical and computer engineering. Since January 1996, he has held a joint appointment in the Department of Biomedical Engineering, Boston University. His research interests are in the areas of multidimensional and multiscale signal and image processing, geometric estimation, detection, and medical signal and image processing.

Prof. Karl has been an Associate Editor of the IEEE TRANSACTIONS ON IMAGE PROCESSING. He has also served in various organizational capacities, including Session Organizer and Chair for the 36th Asilomar Conference on Signals, Systems, and Computers, Special Session on Inverse Problems in Imaging, Session Organizer and Chair for the 2000 Conference in Information Sciences and Systems Special Session on Medical Imaging, and was part of the Organizing Committee for the 1st SIAM Conference on the Life Sciences. He is a member of Sigma Xi.

Bennett B. Goldberg was born in Boston, MA, in 1959. He received the B.A. degree from Harvard College, Cambridge, MA, in 1982 and the M.S. and Ph.D. degrees in physics from Brown University, Providence, RI, in 1984 and 1987, respectively.

Following a Bantrell postdoctoral appointment at the Massachusetts Institute of Technology and the Francis Bitter Magnet Laboratory, Cambridge, he joined the physics faculty at Boston University, in 1989, where he is a Professor of physics and professor of electrical and computer engineering. His active research interests include: near-field imaging of photonic bandgap, ring microcavity and single-mode waveguide devices; subsurface solid immersion microscopy for Si inspection; biosensor fabrication and development of waveguide evanescent bioimaging techniques; magnetooptics and magnetotransport of two- and one-dimensional electron systems; and nanooptics of interacting electron systems in quantum wells and quantum dot structures.

M. Selim Ünlü (M'90–SM'95) was born in Sinop, Turkey, in 1964. He received the B.S. degree in electrical engineering from Middle East Technical University, Ankara, Turkey, in 1986, and the M.S.E.E. and Ph.D. degrees in electrical engineering from the University of Illinois, Urbana–Champaign, in 1988 and 1992, respectively.

In 1992, he joined the Department of Electrical and Computer Engineering, Boston University, Boston, MA, as an Assistant Professor, and has been an Associate Professor since 1998. From January to July 2000, he was a Visiting Professor at University of Ulm, Ulm, Germany. He has authored and coauthored more than 150 technical articles and several book chapters and magazine articles, edited one book, holds one U.S. patent, and has several patents pending. His career interest is in research and development of photonic materials, devices and systems focusing on the design processing, characterization, and modeling of semiconductor optoelectronic devices, especially photodetectors. His current specific interests and expertise include high-speed RCE photodetectors, time and spatially resolved optical characterization of semiconductor materials, near-field and picosecond spectroscopy, near-field imaging of laser diodes, photonic bandgap and guided-wave devices, solid immersion lens microscopy, thermal imaging, biosensor fabrication and development of waveguide evanescent bioimaging techniques, and hyperpolarized noble gas MRI.

Prof. Ünlü served as the Chair of IEEE Laser and Electro-Optics Society, Boston Chapter, from 1994 to 1995, winning the LEOS Chapter-of-the-Year Award. He served as the Vice President of SPIE New England Chapter in 1998–1999. He was awarded the National Science Foundation Research Initiation Award in 1993, the United Nations TOKTEN Award in 1995 and 1996, and both the National Science Foundation CAREER and Office of Naval Research Young Investigator Awards in 1996. From 1999 to 2001, he served as the Chair of the IEEE/LEOS Technical Subcommittee on photodetectors and Imaging and is currently an associate editor for IEEE JOURNAL OF QUANTUM ELECTRONICS.